ISTITUTO NAZIONALE DI FISICA NUCLEARE
Laboratori Nazionali di Frascati

LNF-76/44

A. Del Guerra, A. Giazotto, M. A. Giorgi, A. Stefani,
D. R. Botterill, H. E. Montgomery, P. R. Norton and
G. Matone : THRESHOLD π^+ ELECTROPRODUCTION AT HIGH-MOMENTUM TRANSFER: A DETERMINATION OF THE NUCOEON AXIAL VECTOR FORM FACTOR

Nuclear Phys. B107, 65 (1976)

Servizio Documentazione
dei Laboratori Nazionali di Frascati
Cas. Postale 13 - Frascati (Roma)

Nuclear Physics B107 (1976) 65–81

THRESHOLD π^+ ELECTROPRODUCTION AT HIGH-MOMENTUM TRANSFER: A DETERMINATION OF THE NUCLEON AXIAL VECTOR FORM FACTOR

A. DEL GUERRA, A. GIAZOTTO, M.A. GIORGI and A. STEFANINI
Istituto di Fisica dell'Universita, Pisa
Istituto Nazionale di Fisica Nucleare, Sezione di Pisa, Pisa, Italy

D.R. BOTTERILL, H.E. MONTGOMERY and P.R. NORTON
Daresbury Laboratory, Daresbury, Warrington WA4 4AD, England

G. MATONE
Laboratori Nazionali di Frascati, Rome, Italy

Received 13 February 1976

Threshold π^+ electroproduction has been measured at momentum transfers $|k^2|$ of 0.45, 0.58 and 0.88 $(\mathrm{GeV}/c)^2$, extending the range of earlier measurements. Using PCAC and current algebra-based models we have deduced the axial vector form factor of the nucleon $G_A(k^2)$, and find that the dipole parametrisation is favoured over the monopole. The value of M_A in the dipole parametrisation is, in a weak PCAC model, 0.96 ± 0.03 GeV, in excellent agreement with neutrino measurements. The threshold cross section is also in excellent agreement with the predictions of a fixed-t dispersion relation model.

1. Introduction

Threshold π^+ electroproduction has been studied extensively over the past few years, mainly because of the intimate connection of this process, *via* PCAC and current algebra, with the axial vector form factor of the nucleon, $G_A(k^2)$. (An extensive list of references may be found in ref. [1]). Although G_A may be measured more directly in quasi-elastic neutrino scattering, electroproduction results remain competitive because of their greater statistical precision. Furthermore, the coincidence measurements made at Frascati [2,3], DESY [4] and NINA [1,5] are consistent both amongst themselves and with the neutrino results [6].

We describe in this paper measurements of π^+ threshold electroproduction cross sections at momentum transfers 0.45, 0.58 and 0.88 $(\mathrm{GeV}/c)^2$. These measurements, which extend the $|k^2|$ range previously explored, were performed with essentially the same apparatus used in an earlier experiment [1], where a detailed account of

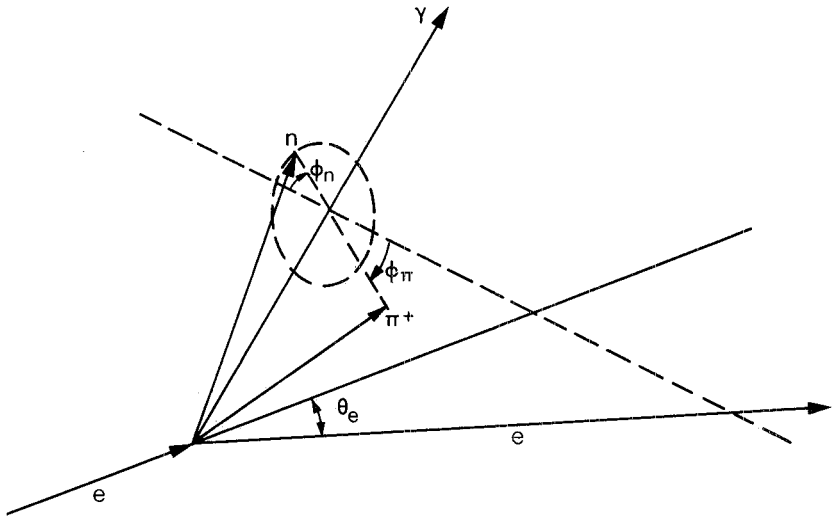

Fig. 1. Kinematic diagram of the reaction, specifying the ϕ convention.

the kinematics and phenomenology may also be found.

The azimuthal differential cross section for $ep \to e\pi^+n$ near threshold may be expanded in powers of q^*, the π^+ momentum in the π^+n c.m.s., as

$$\frac{d^3\sigma}{dE'd\Omega_e d\phi_\pi^*} = \frac{1}{2\pi}\Gamma_t \frac{q^*}{K_L}(A_1 + Bq^{*2} + Cq^{*4} + \tfrac{1}{4}\pi A_4 q^* \cos\phi_\pi^* + \tfrac{2}{3}A_5 q^{*2}\cos 2\phi_\pi^*) . \tag{1}$$

This is an integration over $\cos\theta_\pi^*$ of eq. (3) or ref. [1] with an additional term in q^{*4} which accounts for the d-wave contribution to the total cross section. Γ_t is the virtual photon flux, K_L is the equivalent photon energy given by $(W^2 - M^2)/2M$, with W the invariant mass of the π^+n system and M the proton mass. ϕ_π^* is the azimuthal angle of the π^+ measured about a polar axis in the direction of the virtual photon (see fig. 1).

Integration of eq. (1) over ϕ_π^* gives the total cross section

$$\frac{d^2\sigma}{dE'd\Omega_e} = \Gamma_t \frac{q^*}{K_L}(A_1 + Bq^{*2} + Cq^{*4}) . \tag{2}$$

The dependence on electron variables may be factorised out, and the cross section for virtual photoproduction, $\gamma_v p \to \pi^+ n$, given as

$$\frac{1}{\Gamma_t}\frac{d^3\sigma}{dE'd\Omega_e d\phi_\pi^*} = \frac{d\sigma}{d\phi_\pi^*} = \frac{1}{2\pi}\frac{q^*}{K_L}(A_1 + Bq^{*2} + Cq^{*4} + \tfrac{1}{4}\pi A_4 q^* \cos\phi_\pi^* + \tfrac{2}{3}A_5 q^{*2}\cos 2\phi_\pi^*) . \tag{3}$$

Extrapolation of $(2\pi K_L/q^*)\, d\sigma/d\phi_\pi^*$ to $q^* = 0$ gives the value of A_1, the total cross section slope, which is directly related, through the E_{0+} multipole, to $G_A(k^2)$.

Sect. 2 of this paper contains a brief description of the experimental apparatus, sect. 3 the details of data reduction and analysis, sect. 4 a summary of the cross sections measured; finally in sect. 5 we discuss the results of this and other experiments in relation to G_A.

2. Apparatus and running conditions

The apparatus (fig. 2) has been extensively described in an earlier paper [1], and so we outline here only its basic characteristics and performance and give details of the specific modifications needed for this experiment. The extracted electron beam from the NINA synchrotron was focussed onto a 100 mm long liquid hydrogen target; a dummy target cell was used to measure the background coming from the target walls. The electron beam was measured by a secondary emission monitor (SEM) which had been calibrated separately against a Faraday cup. The scattered electrons were analysed in a focussing magnetic spectrometer whose angular and momentum acceptances were 0.6 msr and 8% respectively. The electron trigger consisted of five scintillation counters, a threshold CO_2 gas Cherenkov counter and a lead-lucite sandwich shower counter. The electron scattering angles and momentum were measured in six scintillation counter hodoscopes. The resolutions

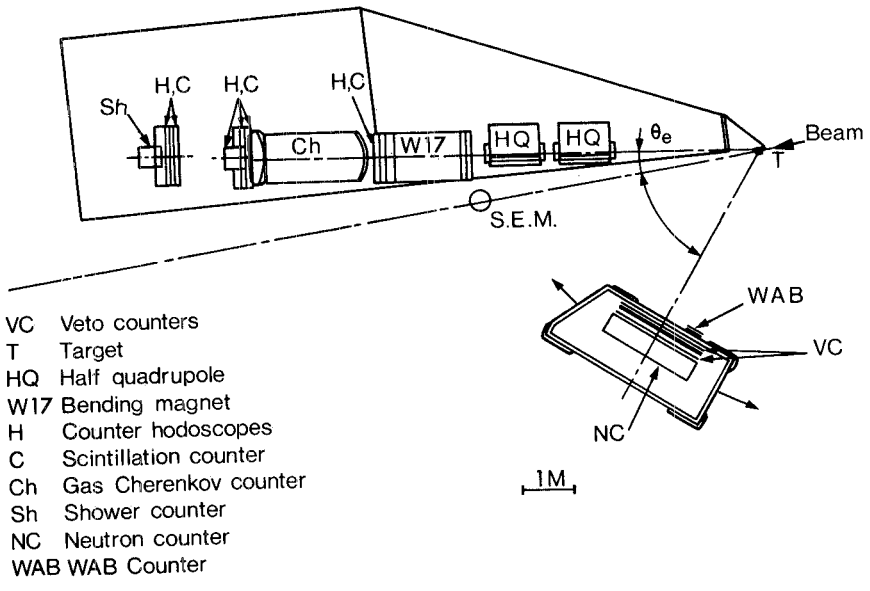

Fig. 2. Lay-out of the experimental apparatus.

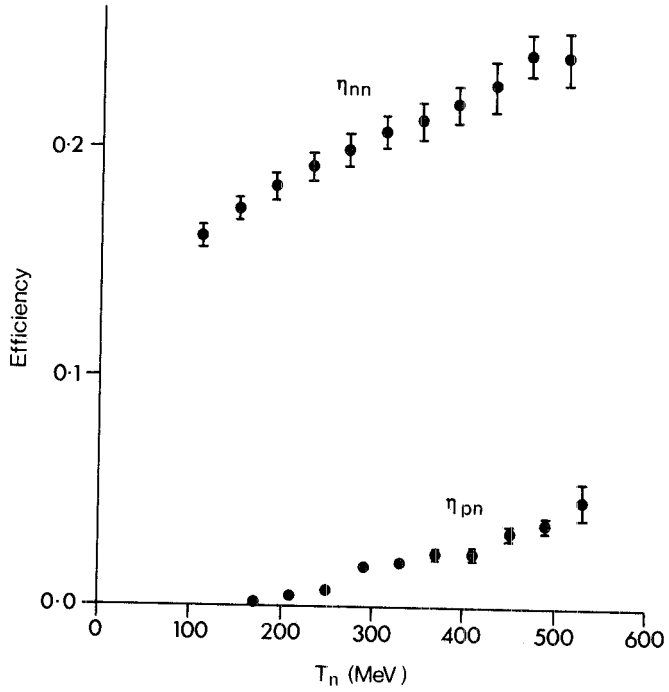

Fig. 3. The efficiency η_{nn} for neutron detection and η_{pn} for proton-neutron conversion.

achieved were ±0.05° in the scattering angle and ±0.3% in $\Delta p/p$. Since the magnetic field of the synchrotron varied sinusoidally, an energy spread of ~1% resulted for electrons incident at different times during the spill (typical length 1.5 ms). For each event the time was recorded relative to the peak of the magnet cycle and the energy calculated.

The experimental determination of the A_1, B and C coefficients of eq. (2) is rather sensitive to the accuracy of the W scale and hence to the absolute value of the incident energy. Whilst the nominal beam energy was recorded event by event, it was known only to an absolute accuracy of ~0.3%. This uncertainty was considerably reduced by performing frequent elastic scattering runs which allowed us to determine the absolute W scale to ±1 MeV.

The electroproduced neutron was determined in a large matrix (NC) of 145 plastic scintillator blocks, each 270 mm deep, encased in a lead shield [7]. The neutron momenta were measured by time of flight (t.o.f.). The efficiency η_{nn} (fig. 3), and the spatial and t.o.f. resolutions of the NC had been carefully measured in the kinetic energy range 100–500 MeV [8].

The single arm (ep → e + anything) trigger clearly allowed several background processes to contribute to the NC signal and each of these had to be carefully handled. Charged and electromagnetic background originating in the target was identified by

means of a veto counter system [1,7] placed in front of the NC and shielded by 50 mm of lead. The veto t.o.f. was also recorded and in the analysis those NC signals with chosen correlations in space and time with the veto signal were designated as "charged" [8,9], e.g. protons from the concurrent process $ep \rightarrow ep\pi^0$. Additional provision was made to handle the background from the process $ep \rightarrow ep\gamma$ (WAB), the radiative tail of elastic ep scattering. This signal dominates the electron trigger near threshold and any misidentification can seriously affect the determination of the π^+ electroproduction. Since the proton distribution from WAB was strongly concentrated over a limited region of the NC, a coincidence telescope (WAB counter) was added, which consisted of two scintillation counters, each 400 × 800 × 10 mm, shielded with 10 mm of iron, the whole assembly bolted to the NC frame (fig. 2). The WAB t.o.f. was also recorded, and was used in the analysis in the same way as the veto counters described earlier. A charged particle was then characterised by giving a signal in either or both of the WAB and veto systems. Despite all these precautions some WAB protons filtered through into the neutral sample *via* conversion in the shielding [8], η_{pn} in fig. 3. A special procedure was developed to handle this much reduced, but still troublesome background (see sect. 3).

Random background was measured by means of a 'random trigger' fanned in with the electron trigger to form the master trigger for the experiment. The random trigger was provided by a small scintillation counter placed beneath the target and properly timed to reproduce the time structure of the beam. The subtraction method has been described in detail elsewhere [9].

The experiment was performed at three different values of the momentum transfer k^2. Table 1 shows the experimental settings together with the other relevant kinematical quantities. The beam intensity was kept fairly high ($\sim 10^{12}$ electrons per second) because of the low cross section of the process.

Table 1
Kinematic settings

$-k^2$ (GeV/c)^2	0.45	0.58	0.88
Incident electron energy E (GeV)	3.198	3.198	3.511
Spectrometer momentum setting E' (GeV/c)	2.754	2.685	2.839
Electron scattering angle θ_e (deg)	13.0	15.0	17.1
Maximum W used in analysis W_{max} (GeV)	1.132	1.144	1.132
Photon polarisation ϵ	0.96	0.95	0.94
Neutron counter angle setting T_n (MeV)	130–330	175–400	270–540
Neutron t.o.f. range τ (ns)	16–35	15–31	14–25
Neutron counter angle setting θ_{NC} (deg)	53.0	50.5	46.5
WAB proton kinetic energy $\bar{T}_p$ (MeV)	~230	~285	~400

3. Data analysis

3.1. Random and dummy subtraction

The data were divided into 45 W bins, each 4 MeV wide, in the range $0.980 \leqslant W \leqslant 1.160$ GeV and 6 ϕ_π^* bins in the range $0^\circ \leqslant \phi_\pi^* \leqslant 180^\circ$ (which also covers the region $180^\circ \leqslant \phi_\pi^* \leqslant 360^\circ$ with the transformation $\phi_\pi^* \to 2\pi - \phi_\pi^*$). The dummy target and random background subtraction were performed in each W and ϕ_π^* bin, plotting the data as a function of the missing mass squared, m^2. To enhance the statistical precision in the subtracted signal a cut was made, typically at $m^2 = -0.08$ GeV^2 and only events above the cut retained. The data at this stage were still contaminated by converted protons from both WAB and $ep \to ep\pi^0$.

3.2. WAB subtraction

The contamination of the neutron yield coming from WAB proton conversion is particularly significant in the $\phi_\pi^* \sim 0^\circ$ region where the WAB proton cone overlaps the neutron cone from π^+ electroproduction. The W spectra of the "neutral sample" coincidence events at $-k^2 = 0.88$ (GeV/c)^2 in the first two ϕ_π^* bins are shown in fig. 4. The physical background below the π^+ threshold (W =1.079 GeV), particularly evident in the first ϕ_π^* bin, can arise only from WAB protons misidentified as neutrons. A similar although less pronounced background is still present in the second ϕ_π^* bin, but in the remaining four bins the signal below threshold was negligible. Unfortunately, the spatial resolution for protons which simulated neutrons had a much longer tail than that for protons detected direct [8]. These two distribution for WAB are therefore markedly different, as can be seen in fig. 5, where the normalised ϕ_n^* ($\equiv \phi_\pi^*$) distributions for protons and for $p \to n$ conversions are shown in the W region below threshold (e.g. the ratio between bin 2 and bin 1 is 0.03 for protons and 0.36 for $p \to n$). This prevented us from handling the $p \to n$ conversion by directly subtracting an appropriate measured fraction (η_{pn} in fig. 3) of the charged yield from the neutral yield. To overcome this difficulty a Monte-Carlo program was used to simulate the WAB proton distribution on the NC. The goodness of this simulation was checked against the measured WAB proton distribution below threshold using the known efficiency of the NC for detecting protons (~67% with a cut-off at ~290 MeV [8]. The generated distribution was then multiplied by the $p \to n$ conversion efficiency η_{pn} and smeared using the measured spatial resolution for $p \to n$ detection [8]. The six W distributions obtained were individually normalised to give the experimentally observed yield of neutrons in the W range $1.024 \leqslant W \leqslant 1.064$ GeV (immediately below threshold), and were then subtracted from the measured yields. The Monte Carlo yields for WAB are shown in fig. 4, together with the data. As can be seen, the experimental shape in W below threshold is well reproduced by the Monte Carlo. We estimate that the maximum error arising from this subtraction is less than 10% in the first ϕ_π^* bin, less than 3% in the second, and negligible in the remaining

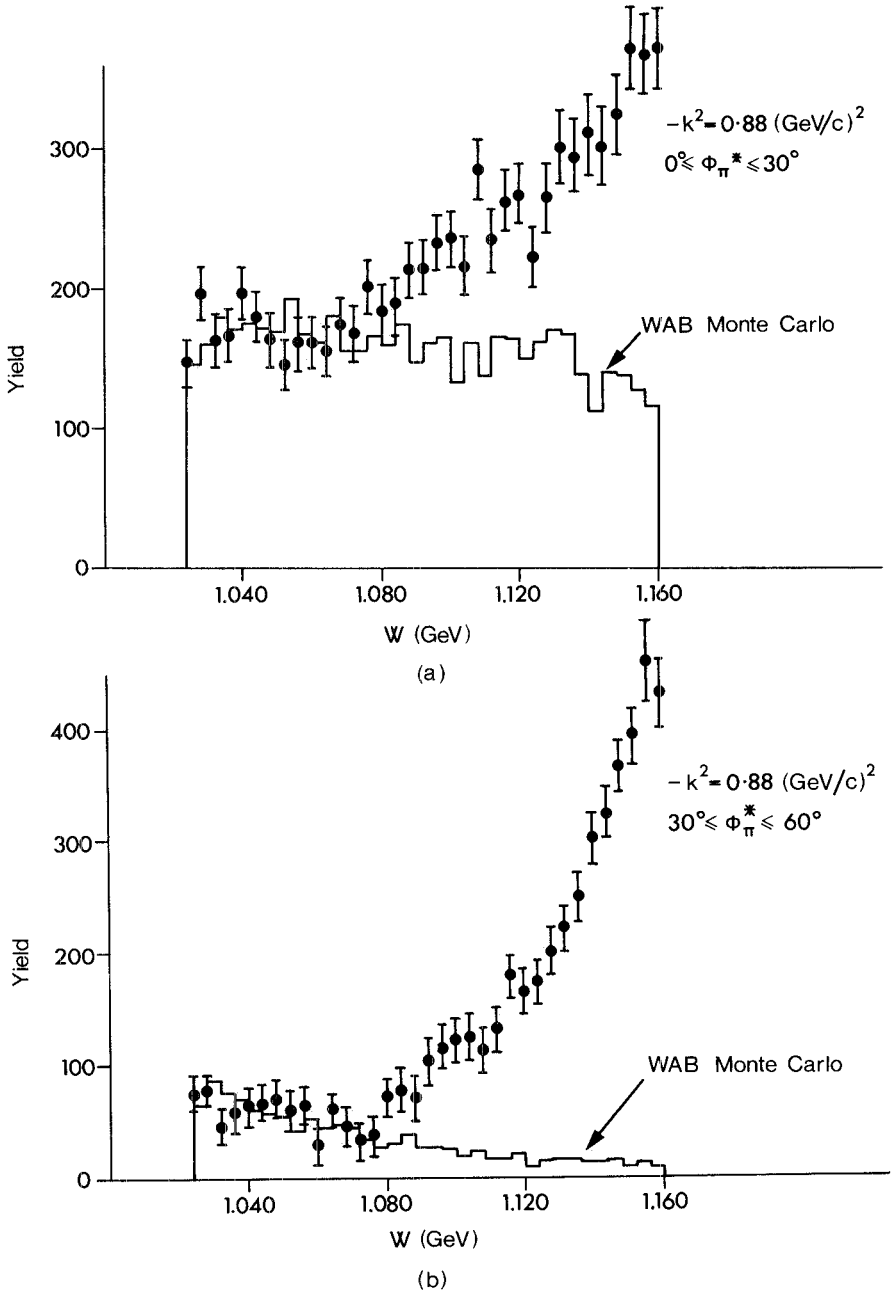

Fig. 4. Experimental yields as a function of W. (a) $0° \leqslant \phi_\pi^* \leqslant 30°$. (b) $30° \leqslant \phi_\pi^* \leqslant 60°$. The yield from WAB, as calculated by Monte Carlo, is also shown.

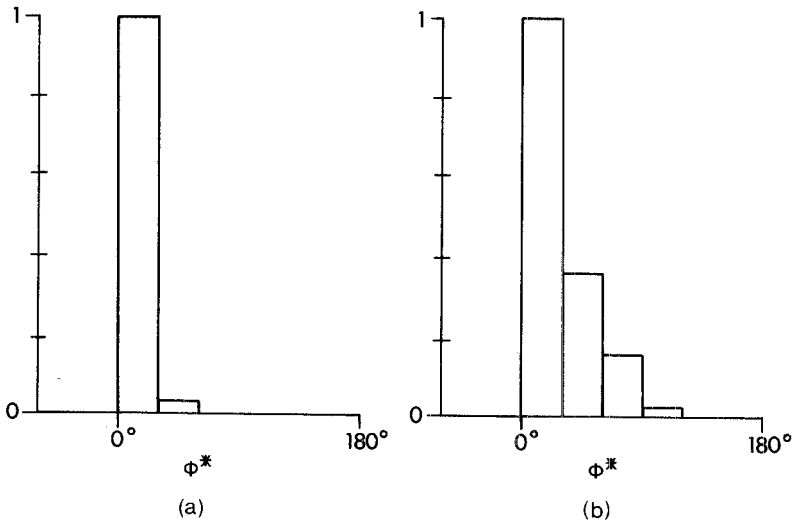

Fig. 5. The ϕ^* distributions for protons from WAB. (a) Protons detected direct. (b) Protons detected *via* p → n conversion.

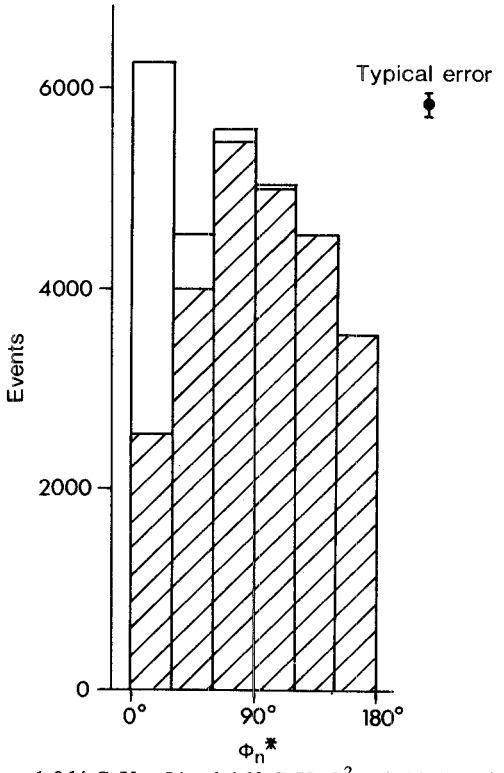

Fig. 6. The ϕ_π^* distribution, 1.064 GeV $\leqslant W \leqslant$ 1.160 GeV, $|k^2| = 0.88$ (GeV/c)^2 for ep → eπ^+n. The shaded region is the distribution after the removal of the WAB contamination.

four. The W-integrated ϕ histograms ($1.064 \leqslant W \leqslant 1.160$ GeV), before and after WAB subtraction, are shown in fig. 6 at $-k^2 = 0.88$ (GeV/c)^2. After subtraction there is a clear asymmetry between $\phi_n^* = 0°$ and $\phi_\pi^* = 180°$, giving rise to a large and negative A_4 coefficient in the differential cross section (eq. 3), which was completely masked before subtraction by the WAB proton contamination.

3.3. $\pi^0 p$ contamination and cross-section evaluation

The procedure used for the analysis was very similar to that described in ref. [1]. A Monte-Carlo program, incorporating the effects of both internal and external radiation, was used to simulate π^+n electroproduction. Each simulated event was labelled with a set of generated variables $\alpha(\equiv W, \cos\theta_\pi^*, \theta_\pi^*, T_n)$, where T_n is the neutron kinetic energy, and a set of reconstructed variables $\alpha'(\equiv W', \phi_\pi^{*\prime})$. The following quantities were then calculated:

$$D_1^+(\alpha') = \sum_{\text{MC events}} W_j^+(\alpha',\alpha)\, H^+(\alpha)\, \eta_{nn}(T_n)\,,$$

$$D_4^+(\alpha') = \sum_{\text{MC events}} W_j^+(\alpha',\alpha)\, H^+(\alpha)\, \eta_{nn}(T_n)\, q^{*}\tfrac{1}{4}\pi \cos\phi_\pi^*\,,$$

$$D_5^+(\alpha') = \sum_{\text{MC events}} W_j^+(\alpha',\alpha)\, H^+(\alpha)\, \eta_{nn}(T_n)\, q^{*2}\tfrac{2}{3}\cos 2\phi_\pi^*\,,$$

$$D_B^+(\alpha') = \sum_{\text{MC events}} W_j^+(\alpha',\alpha)\, H^+(\alpha)\, \eta_{nn}(T_n)\, q^{*2}\,,$$

$$D_C^+(\alpha') = \sum_{\text{MC events}} W_j^+(\alpha',\alpha)\, H^+(\alpha)\, \eta_{nn}(T_n)\, q^{*4}\,, \qquad (4)$$

where $W_j^+(\alpha',\alpha)$ is the weight of the jth Monte-Carlo event and $H^+(\alpha)$ is the input cross section to the Monte Carlo, flat in $\cos\theta_\pi^*$ and ϕ_π^* and giving $(K_L/q^*)(d\sigma/d\phi_\pi^*)$ a flat behaviour in W and ϕ_π^*. Since we do not present any distributions in $\cos\theta_\pi^*$, the Monte-Carlo events were integrated over this variable.

To remove the physical background produced by the process $ep \to ep\pi^0$ with the proton misidentified as a neutron in the NC, the further set of quantities below was evaluated with the same Monte-Carlo program

$$D_1^0(\alpha') = \sum_{\text{MC events}} W_j^0(\alpha',\alpha)\, H^0(\alpha)\, \eta_{pn}(T_p)\,,$$

$$D_2^0(\alpha') = \sum_{\text{MC events}} W_j^0(\alpha',\alpha)\, H^0(\alpha)\, \eta_{pn}(T_p)\, q^* \cos\theta_{\pi 0}^*\,,$$

$$D_3^0(\alpha') = \sum_{\text{MC events}} W_j^0(\alpha',\alpha)\, H^0(\alpha)\, \eta_{pn}(T_p)\, q^{*2} \cos^2\theta_{\pi 0}^*\,,$$

$$D_4^0(\alpha') = \sum_{\text{MC events}} W_j^0(\alpha',\alpha)\, H^0(\alpha)\, \eta_{pn}(T_p)\, q^* \sin\theta_{\pi 0}^* \cos\phi_{\pi 0}^*\,,$$

$$D_5^0(\alpha') = \sum_{\text{MC events}} W_j^0(\alpha', \alpha)\, H^0(\alpha)\, \eta_{\text{pn}}(T_\text{p})\, q^{*2} \sin^2\theta^*_{\pi 0} \cos 2\phi^*_{\pi 0} ,$$

$$D_B^0(\alpha') = \sum_{\text{MC events}} W_j^0(\alpha', \alpha)\, H^0(\alpha)\, \eta_{\text{pn}}(T_\text{p})\, q^{*2} ,$$

$$D_C^0(\alpha') = \sum_{\text{MC events}} W_j^0(\alpha', \alpha)\, H^0(\alpha)\, \eta_{\text{pn}}(T_\text{p})\, q^{*4} , \qquad (5)$$

where W_j^0 and H^0 are evaluated for the pπ^0 final state. Unlike the π^+ [eq. (4)], for the π^0 we had to account for the cos $\theta^*_{\pi 0}$ because of the evident strong dependence of η_{np} on the proton energy (fig. 3). The yield of converted protons is then given by

$$D^0(\alpha') = \sum D_i^0(\alpha')\, A_i^0 + D_B^0(\alpha')\, B^0 + D_C^0(\alpha')\, C^0 , \qquad (6)$$

where A_i^0, B^0 and C^0 are the coefficients of an expansion of the π^0p cross section analogous to eq. (3). At $-k^2 = 0.45$ and 0.58 (GeV/c)^2 these coefficients were computed using a theoretical model [10], whilst at $-k^2 = 0.88$ the coefficients A_1^0, A_4^0, A_5^0, B^0 and C^0 were experimentally measured and the A_2^0 and A_3^0 inserted from the same model. The contribution $D^0(\alpha')$ of the π^0 contamination to the total neutron yield was 5.5%, 10% and 15% at the three settings 0.45, 0.58 and 0.88 (GeV/c)^2, respectively. At the highest $|k^2|$, where the correction was highest, $D^0(\alpha')$ is almost model independent, whereas at the two lower $|k^2|$ values we estimate an uncertainty of ~2% from the model used. A second theoretical model [11] gives predictions within this estimated error.

The π^+n coefficients A_1, A_4, A_5, B and C of eq. (3) were obtained by minimising the χ^2 between the binned experimental yield and the quantity

$$D^{\text{tot}}(\alpha') = D_1^+(\alpha')\, A_1 + D_4^+(\alpha')\, A_4 + D_5^+(\alpha') A_5 + D_B^+(\alpha') B + D_C^+(\alpha')\, C + D^0(\alpha') . \qquad (7)$$

3.4. Corrections

The following normalisation corrections were applied to the data:
(i) Electron reconstruction efficiency (11%). [1].
(ii) Accidental vetoing of neutrons by WAB or veto counters (~2%).
(iii) Trigger inefficiency (4%).

4. Results

In fig. 7 we show the values of the A_1 coefficient (the threshold cross-section slope) together with the results of the earlier NINA experiment [1] and those from DESY [4]. We also show the predictions of the fixed-t dispersion relation

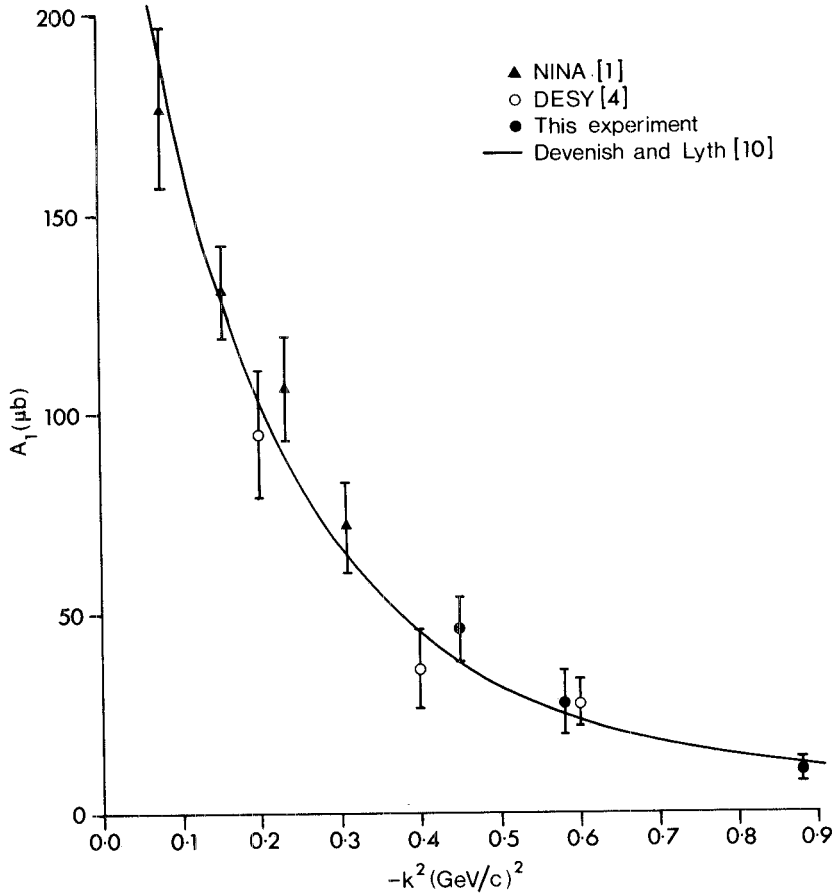

Fig. 7. The threshold cross-section slope, A_1.

model of Devenish and Lyth [10] which is seen to be in excellent agreement with the data over the whole k^2 range. The Frascati results [2,3] have not been presented here because their polarisation ϵ was significantly lower (~0.75) and the comparison is not necessarily valid.

The q^{*2} coefficient B is shown in fig. 8a, with the predictions of Devenish and Lyth [10], and also of the pseudovector Born approximation of Dombey and Read [11]. There is good agreement between the models and the present data and this confirms the assumptions made in the analysis of the earlier experiment [1], in which B could not be measured directly, but had to be taken from these same models in order to evaluate A_1.

The q^{*4} coefficient C is shown in fig. 8b. It is negative at all $|k^2|$ values. The two models are in substantial agreement with the data, but it should be pointed out that the predictions for C are sensitive to the W range used, and precise comparisons are difficult.

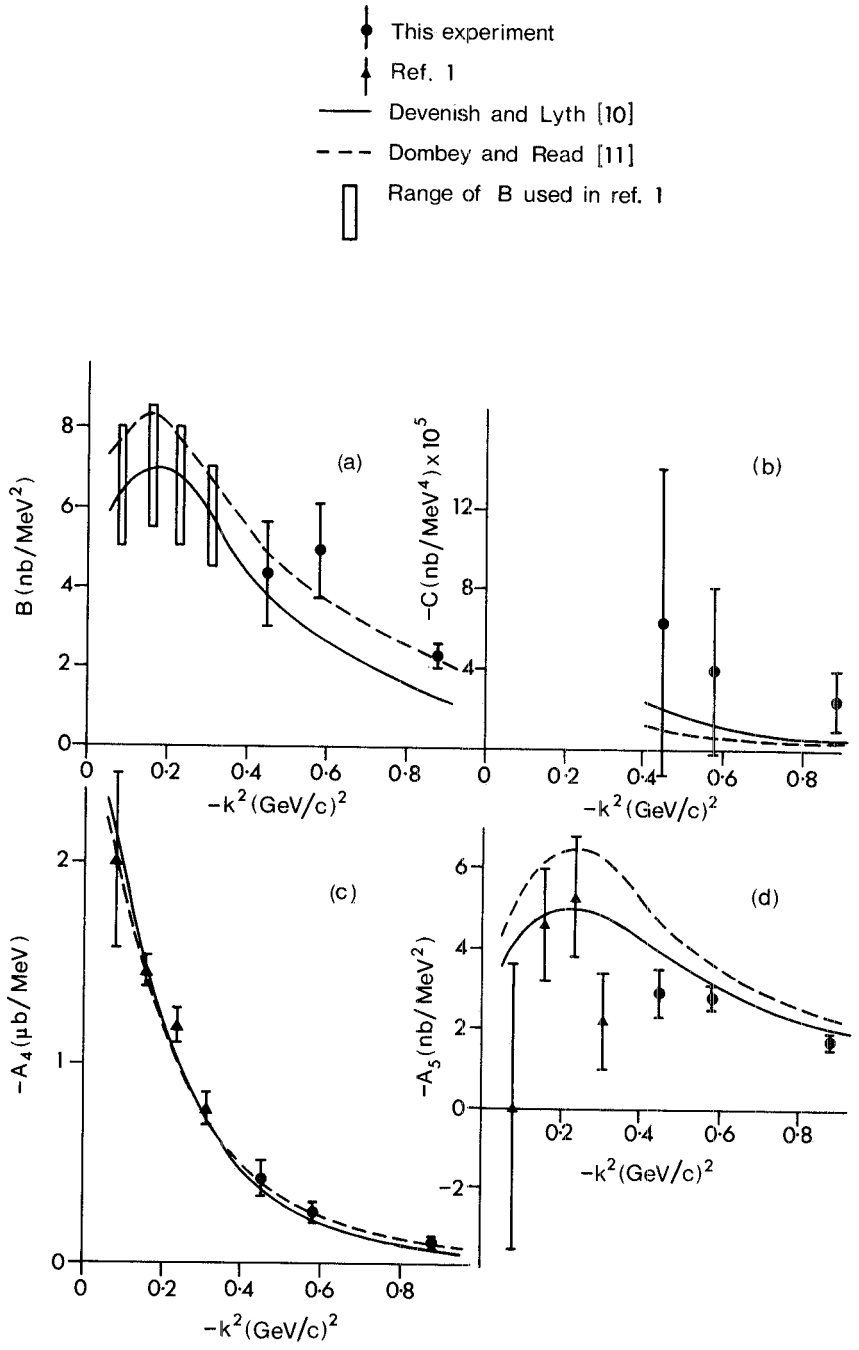

Fig. 8. Comparison of the coefficients B, C, A_4 and A_5 with ref. [1] and with models.

The A_4 and A_5 coefficients are shown in figs. 8c and 8d, together with the measurements of ref. [1] and the predictions of the same two models. Both models are in excellent agreement with the measurements, in particular with A_4.

The measured coefficients at the three $|k^2|$ values are summarised in table 2. The errors quoted are the combination in quadrature of the statistical error, ranging between 15% at the lowest $|k^2|$ and 20% at the highest (including the correlation between the various coefficients) and a systematic error of ~10–20% arising chiefly from the uncertainty in the incident electron energy (±1 MeV).

We show in table 3 the values of $G_A(k^2)/G_A(0)$ deduced from this experiment using three different models, the 'weak PCAC' model of Benfatto, Nicolò and Rossi (BNR) [12], the pseudovector Born approximation of Dombey and Read [11], and the exact soft pion limit [13]. The model of Furlan, Paver and Verzegnassi (see ref. [1]) has not been used since it is not expected to be valid in our $|k^2|$ range. We show also the results of fitting G_A to a dipole ($n = 2$) or monopole ($n = 1$) form

$$\frac{G_A(k^2)}{G_A(0)} = \left(1 + \frac{|k^2|}{M_A^2}\right)^{-n}.$$

Table 2
Cross-section coefficients measured in this experiment

$-k^2$(GeV/c)^2	0.45	0.58	0.88
A_1 (μb)	46.1 ± 8.2	27.4 ± 8.0	10.6 ± 2.8
B (nb/MeV^2)	4.3 ± 1.3	4.9 ± 1.2	2.3 ± 0.3
C (nb/MeV^4)	(− 6.4 ± 7.7)10^{-5}	(− 4.0 ± 4.1)10^{-5}	(− 2.5 ± 1.5)10^{-5}
A_4(μb/MeV)	− 0.43 ± 0.09	− 0.26 ± 0.05	− 0.11 ± 0.02
A_5 (nb/MeV^2)	− 2.9 ± 0.6	− 2.9 ± 0.6	− 1.7 ± 0.2

Table 3
$G_A(k^2)/G_A(0)$ deduced from this experiment

	BNR	DR	Soft-pion limit
$-k^2$ = 0.45 (GeV/c)^2	$0.495^{+0.045}_{-0.050}$	$0.562^{+0.039}_{-0.042}$	$0.538^{+0.034}_{-0.036}$
$-k^2$ = 0.58 (GeV/c)^2	$0.390^{+0.055}_{-0.080}$	$0.462^{+0.050}_{-0.061}$	$0.450^{+0.043}_{-0.049}$
$-k^2$ = 0.88 (GeV/c)^2	$0.245^{+0.040}_{-0.070}$	$0.321^{+0.025}_{-0.029}$	$0.317^{+0.025}_{-0.027}$
Dipole fit M_A (GeV)	0.99 ± 0.06	1.10 ± 0.04	1.08 ± 0.04
Monopole fit M_A (GeV)	0.62 ± 0.04	0.69 ± 0.04	0.68 ± 0.03

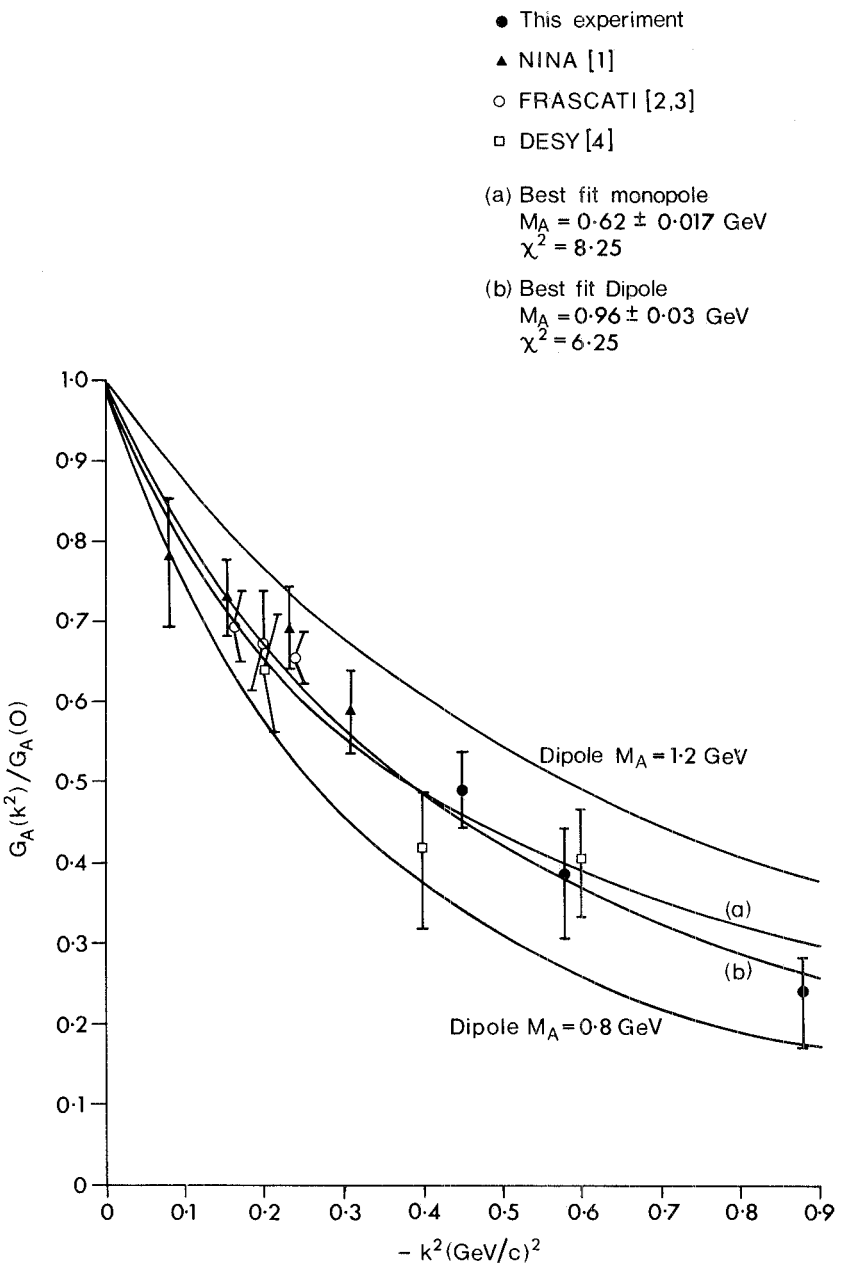

Fig. 9. $G_A(k^2)/G_A(0)$ deduced using the Benfatto-Nicolò-Rossi model [12]. The best fits to a dipole and monopole parametrisation are shown.

We note that the DR model gives values of G_A considerably higher than that of BNR, and a little higher than the soft-pion limit. The same behaviour was observed in comparison with low $|k^2|$ measurements [1].

5. Conclusions

We have performed a fit to all data on threshold π^+ electroproduction using the data of refs. [1–4] in addition to these new measurements, assuming that G_A is either dipole or monopole in form. The fits for the BNR model [12] are shown in fig. 9. The 'dipole' M_A is 0.96 ± 0.03 GeV and the dipole is preferred over the monopole form. The Dombey and Read model gives a dipole M_A of 1.12 ± 0.03 GeV.

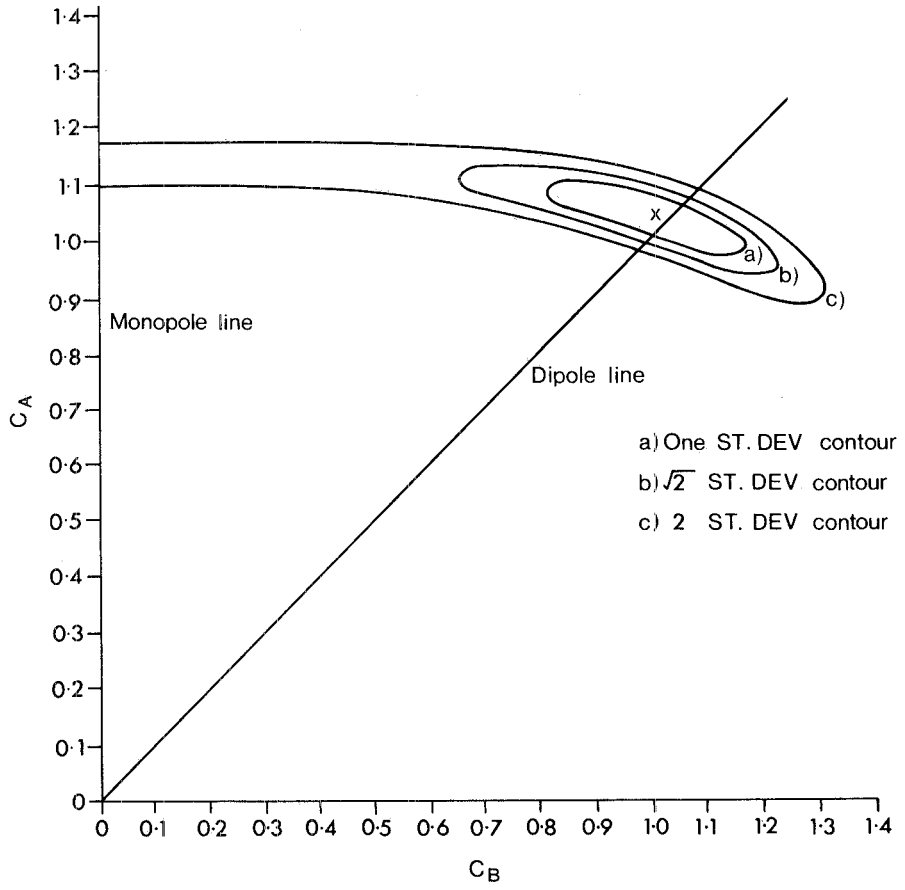

Fig. 10. χ^2 contours for the fit described in the text, showing the preference for a dipole over a monopole parametrisation.

We make the observation here that the most recently quoted results from quasi-elastic neutrino scattering [14] give dipole fits to M_A of 0.84 ± 0.11 GeV from the differential cross section and M_A = 0.98 ± 0.13 GeV from the total cross section, an average of 0.89 ± 0.08 GeV. We therefore conclude that excellent agreement is obtained between the neutrino and electroproduction measurements when the Benfatto-Nicolò-Rossi model is used, whereas the agreement is far less satisfactory with the Dombey-Read model.

We have investigated further in the BNR model the dipole and monopole fits. The measurement at $|k^2| = 0.88$ (GeV/c)^2 allows the possibility of distinguishing if either is preferred. We have fitted the function

$$\frac{G_A(k^2)}{G_A(0)} = \frac{1}{1 + 2C_A^2|k^2| + C_B^4|k^2|^2}$$

and evaluated the best-fit values of C_A and C_B. If $C_A = C_B$ the function is simply the dipole, and if $C_B = 0$ it is the monopole. The best fit, shown in fig. 10 is in very striking agreement with the dipole, i.e. $C_A = C_B$. However, as can be seen from the χ^2 contours, the monopole is not rejected at the level of 1.5 standard deviations.

To summarise, by extending the measured range of $|k^2|$ in threshold π^+ electroproduction to 0.88 (GeV/c)^2 we have improved the measurement of M_A, and we have shown that G_A is better represented by a dipole than a monopole formula.

We should like to express our thanks to Professors A. Ashmore, A. Donnachie, and to Dr. J. Bailey for their support and encouragement, to D. Clarke, K. Connell and P. Salvadori for their excellent technical support throughout, and to Drs. G. Benfatto, B.J. Read and R.C.E. Devenish for discussions and communication of their predictions. We also wish to thank the NINA crew and the Daresbury Laboratory engineering support staff for all their helpful cooperation.

References

[1] A. Del Guerra, A. Giazotto, M.A. Giorgi, A. Stefanini, D.R. Botterill, D.W. Braben, D. Clarke and P.R. Norton, Nucl. Phys. B99 (1975) 253.
[2] E. Amaldi, B. Borgia, P. Pistilli, M. Balla, G.V. Di Giorgio, A. Giazotto, S. Serbassi and G. Stoppini, Nuovo Cimento 65A (1970) 377.
[3] E. Amaldi, M. Beneventano, B. Borgia, F. De Notaristefani, A. Fronderoli, P. Pistilli, I. Sestili and M. Severi, Phys. Letters 41B (1972) 216.
[4] P. Brauel, F.W. Büsser, Th. Canzler, D. Cords, W.R. Dix, R. Felst, G. Grindhammer, W.D. Kollman, H. Krehbiel, J. Meyer and G. Weber, Phys. Letters 45B (1973) 389; 50B (1974) 507.
[5] D.R. Botterill, D.W. Braben, R. Kikuchi, P.R. Norton, A. Del Guerra, A. Giazotto, M.A. Giorgi and A. Stefanini, Phys. Letters 45B (1973) 405.
[6] G. Weber, DESY Report 75/17, EPS Int. Conf. on high-energy physics, Palermo 1975.

[7] A. Del Guerra, A. Giazotto, M.A. Giorgi, A. Stefanini, D.R. Botterill, D.W. Braben, D. Clarke and P.R. Norton, Daresbury Laboratory, preprint DL/P260 (1976).
[8] J. Bailey, D.R. Botterill, D. Clarke, H.E. Montgomery, P.R. Norton, G. Matone, A. Del Guerra, A. Giazotto, M.A. Giorgi and A. Stefanini, Daresbury Laboratory preprint, DL/P 255 (1976).
[9] J. Bailey, D.R. Botterill, D.W. Braben, D. Clarke, H.E. Montgomery, P.R. Norton, G. Matone, A. Del Guerra, A. Giazotto, M.A. Giorgi and A. Stefanini, Daresbury Laboratory preprint DL/P253 (1975).
[10] R.C.E. Devenish and D.H. Lyth, Nucl. Phys. B93 (1975) 109 and private communication.
[11] N. Dombey and B.J. Read, Nucl. Phys. B60 (1973) 65;
B.J. Read, Nucl. Phys. B74 (1974) 482, and private communication.
[12] G. Benfatto, F. Nicolò and G.C. Rossi, Nucl. Phys. B50 (1972) 205; Nuovo Cimento 14A (1973) 425;
G. Benfatto, private communication.
[13] Y. Nambu and M. Yoshimura, Phys. Rev. Letters 24 (1970) 25.
[14] S.J. Barish et al., quoted by D.H. Perkins, Invited talk, 7th Int. Symp. on lepton and photon interactions, Stanford 1975.